Enhancing Oxygen Reduction Reaction Activity in ZIF-Derived Catalysts through Thermal Oxidation-Induced Micropore Enlargement

Yu Joong Kim[a,1], Ki Hwan Koh[b,1], Hyeong Jun Kim[a], Hyeonhoo Lee[a], Sima Umrao[a], Youn Jeong Jang[c,], and Tae Hee Han[a,d,*]*

[a] Department of Organic and Nano Engineering, Human-Tech Convergence Program, Hanyang University, Seoul 04763, Republic of Korea

[b] Advanced Battery Research Center, Division of Advanced Materials, Korea Research Institute of Chemical Technology, 141 Gajeong-ro, Yuseong-gu, Daejeon 34114, Republic of Korea

[c] Department of Chemical Engineering, Hanyang University, Seoul 04763, Republic of Korea

[d] The Research Institute of Industrial Science, Hanyang University, Seoul 04763, Republic of Korea

E-mail: than@hanyang.ac.kr (T. H. Han); yjang53@hanyang.ac.kr (Y. J. Jang)

[1] These two authors contributed equally to this work.

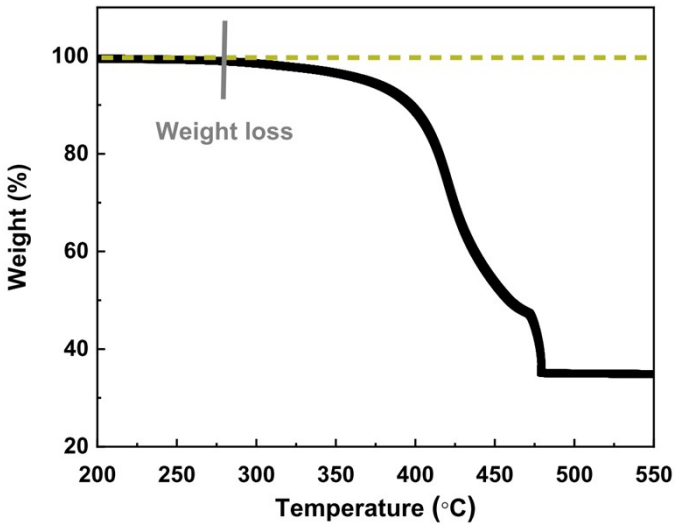

Figure. S1. TGA curves of Zn, Co-ZIF.

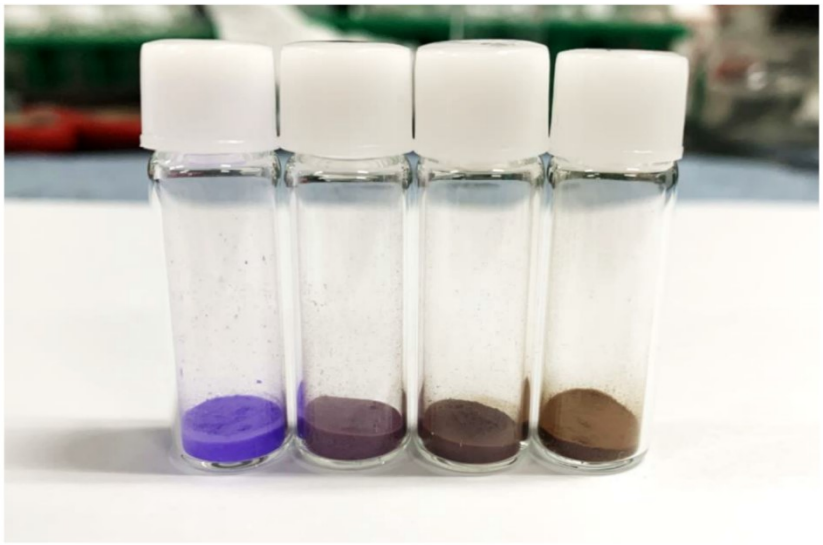

Figure. S2. The images of Zn, Co-ZIF, O-ZIF@280, O-ZIF@310, and O-ZIF@340 from left to right.

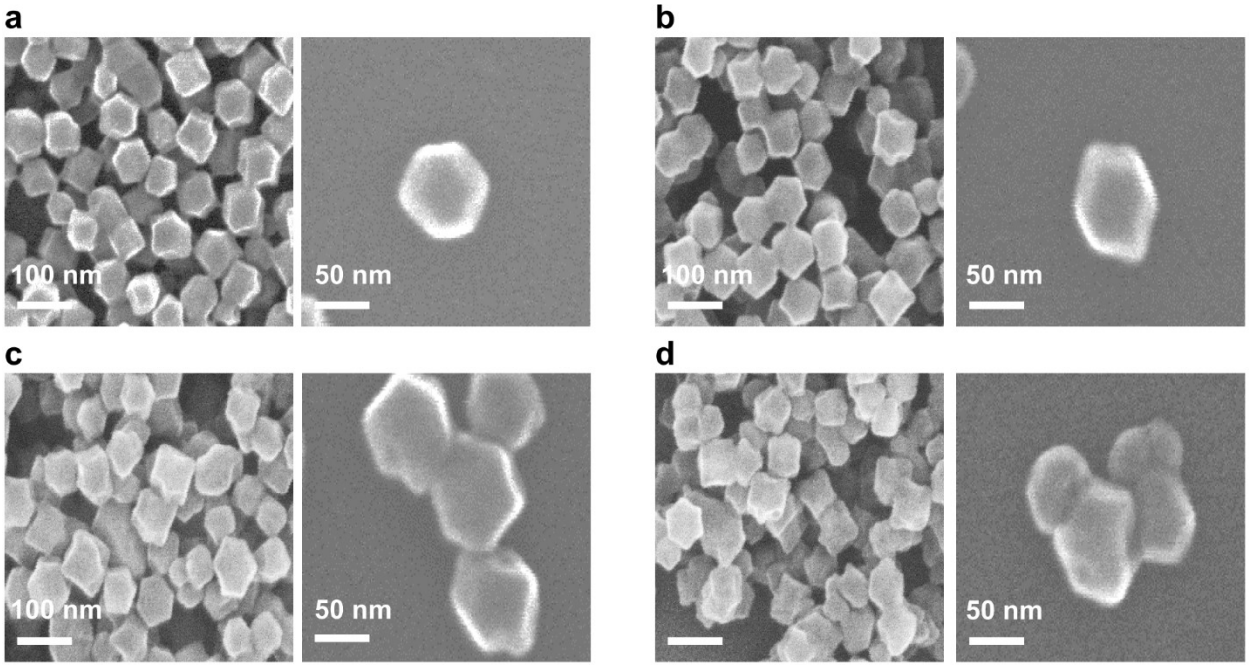

Figure. S3. (a, b, c, d) SEM images of Zn, Co-ZIF, O-ZIF@280, O-ZIF@310, O-ZIF@340, respectively.

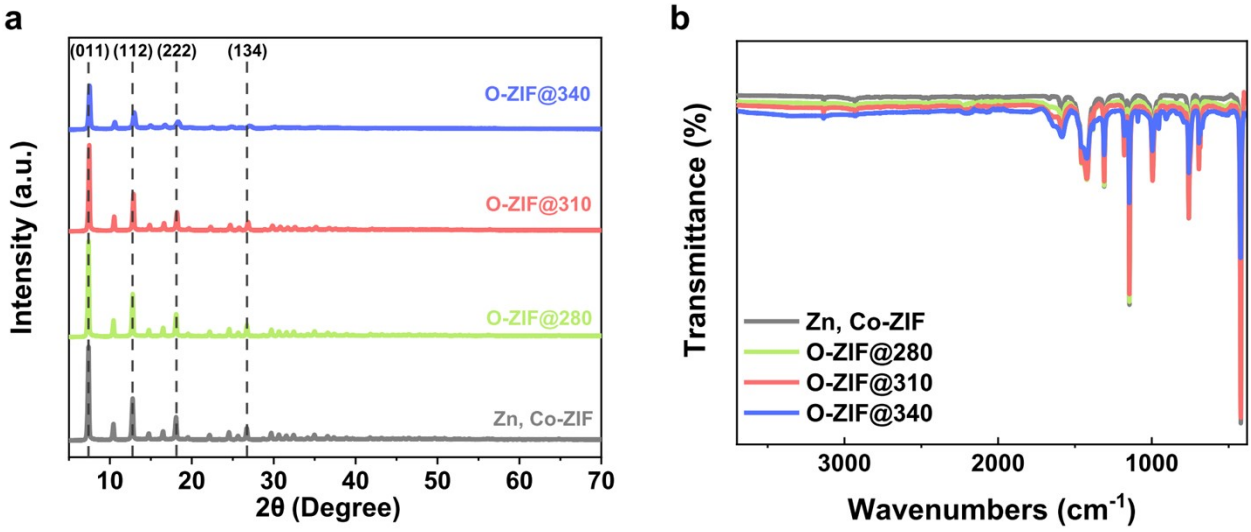

Figure. S4. (a) XRD patterns; (b) FT-IR spectra of oxidized ZIF series.

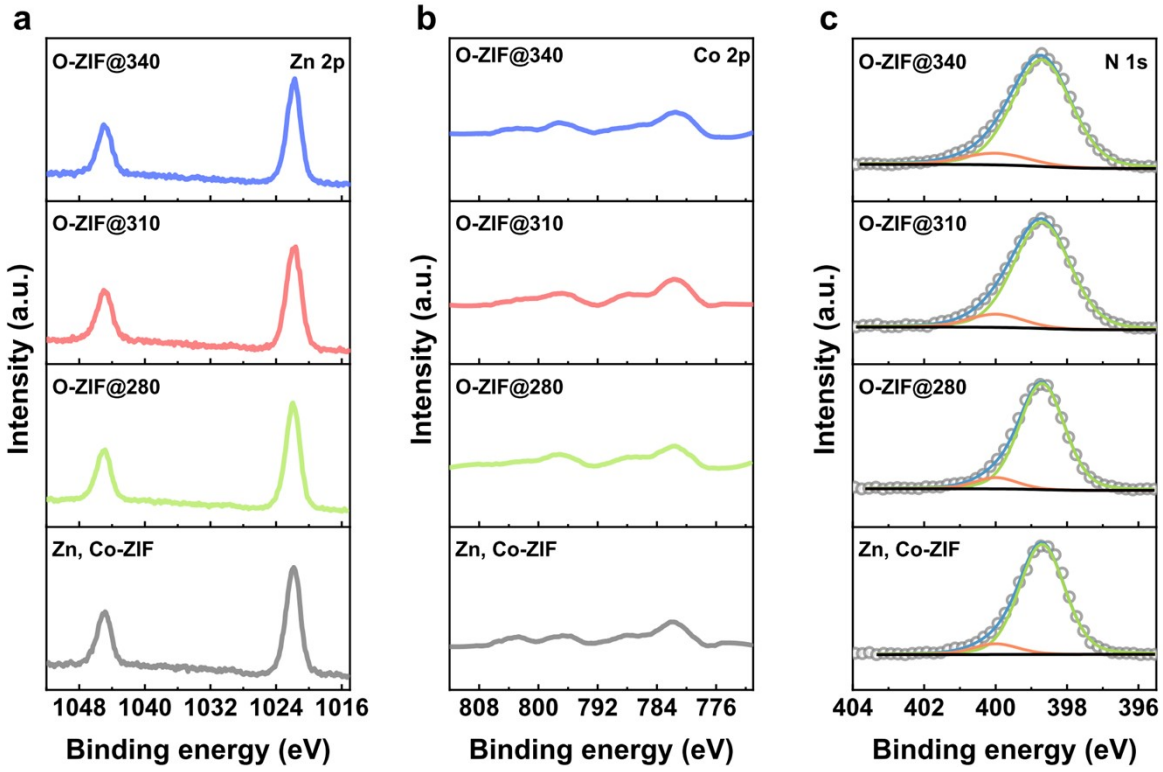

Figure. S5. XPS spectra of (a) Zn 2p, (b) Co 2p, and (c) N 1s of Zn, Co-ZIF and oxidized ZIFs**.**

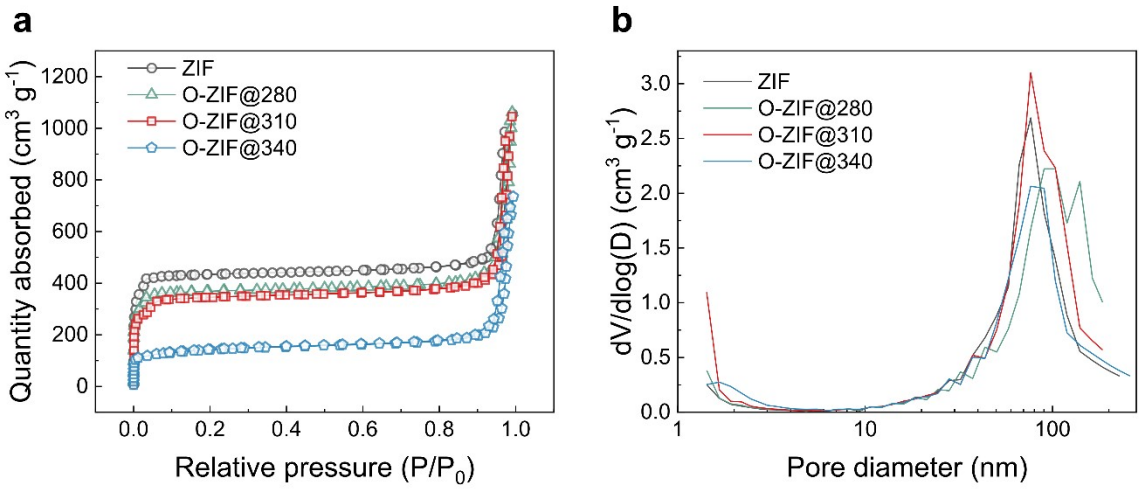

Figure. S6. (a) N_2 adsorption–desorption isotherms; (f) corresponding pore size distribution.

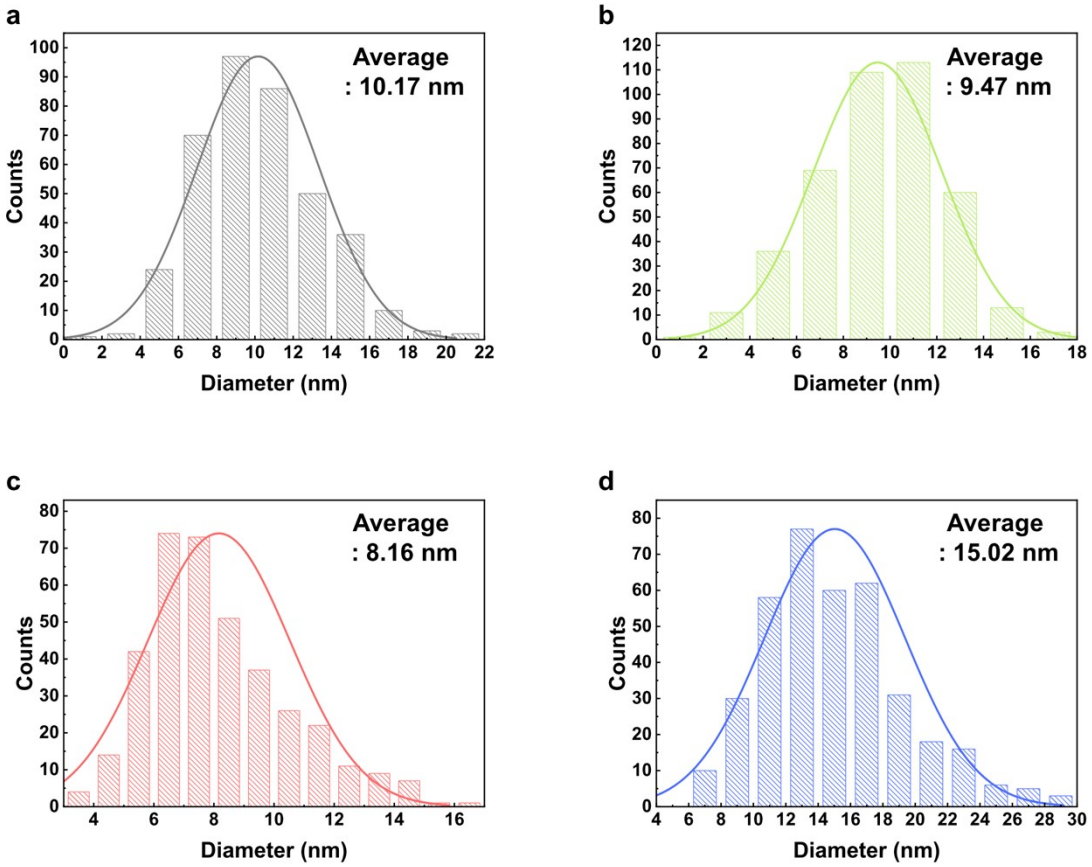

Figure. S7. a,b,c,d, Size distribution of Co nanoparticles of (a) Co/N-C_1, (b) Co/N-C_2, (c) Co/N-C_3, and (d) Co/N-C_4.

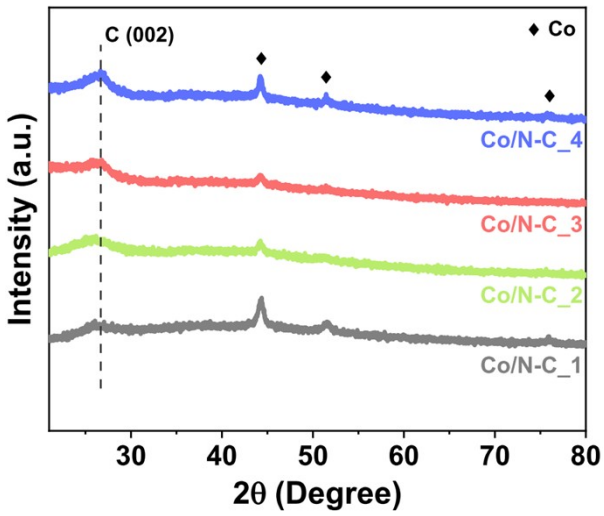

Figure. S8. XRD pattern Co/N-C series.

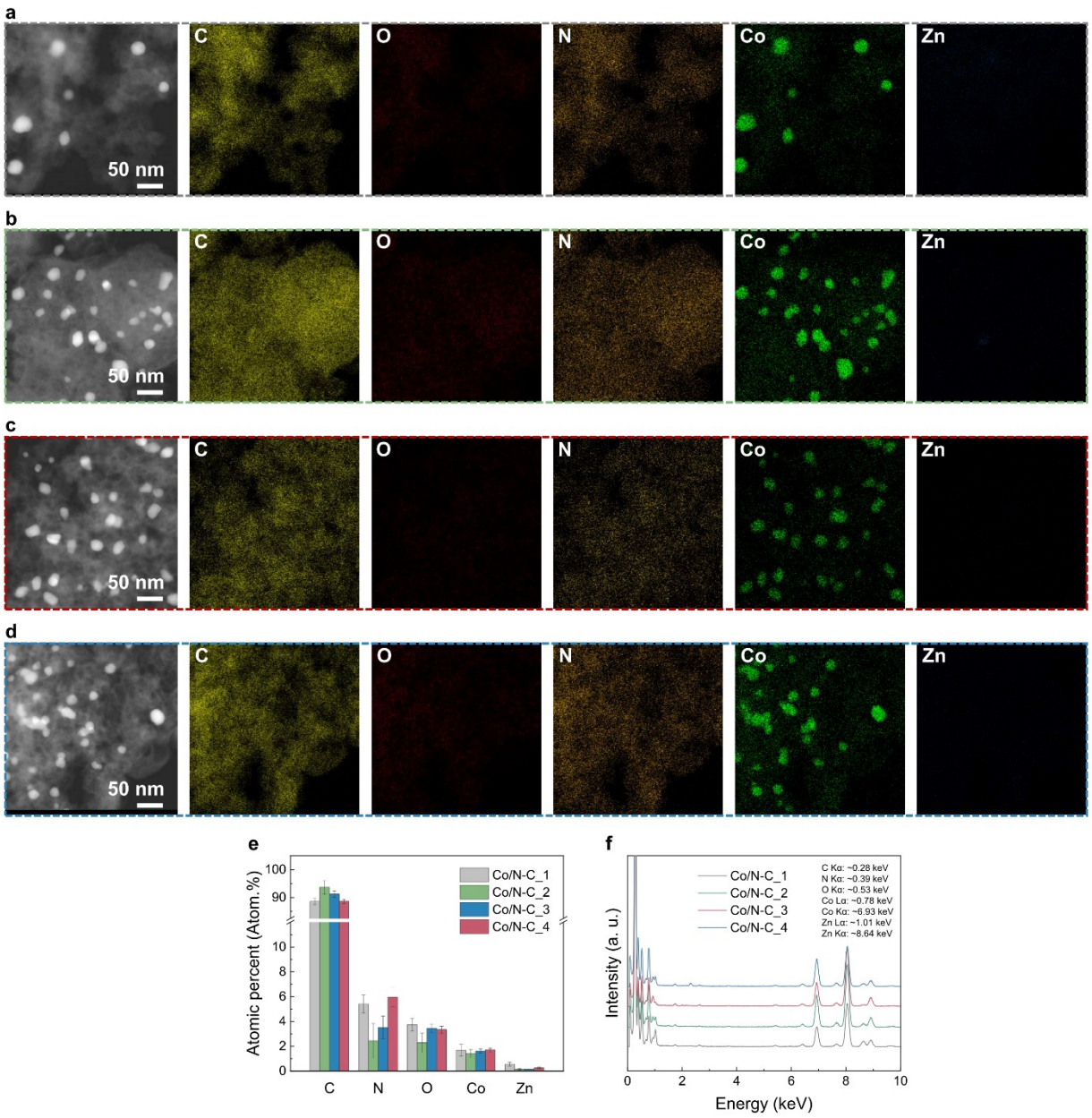

Figure. S9. Corresponding EDS mapping of (a) Co/N-C_1, (b) Co/N-C_2, (c) Co/N-C_3, (d) Co/N-C_4, (e) summerized results and (f) spectra for all the samples.

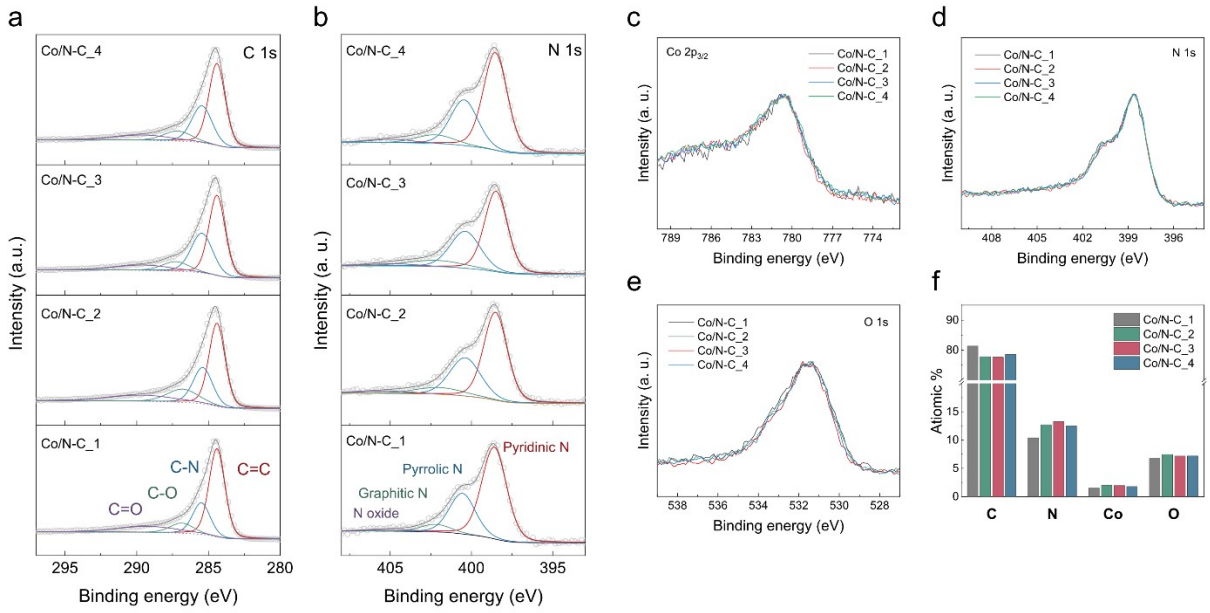

Figure. S10. XPS spectra of (a) C 1s, (b) N 1s, and normalized spectra of (c) Co 2p; (d) N1s, (e) O1s, and (f) the atomic ratio of C, N, Co, and O in Co/N-C series.

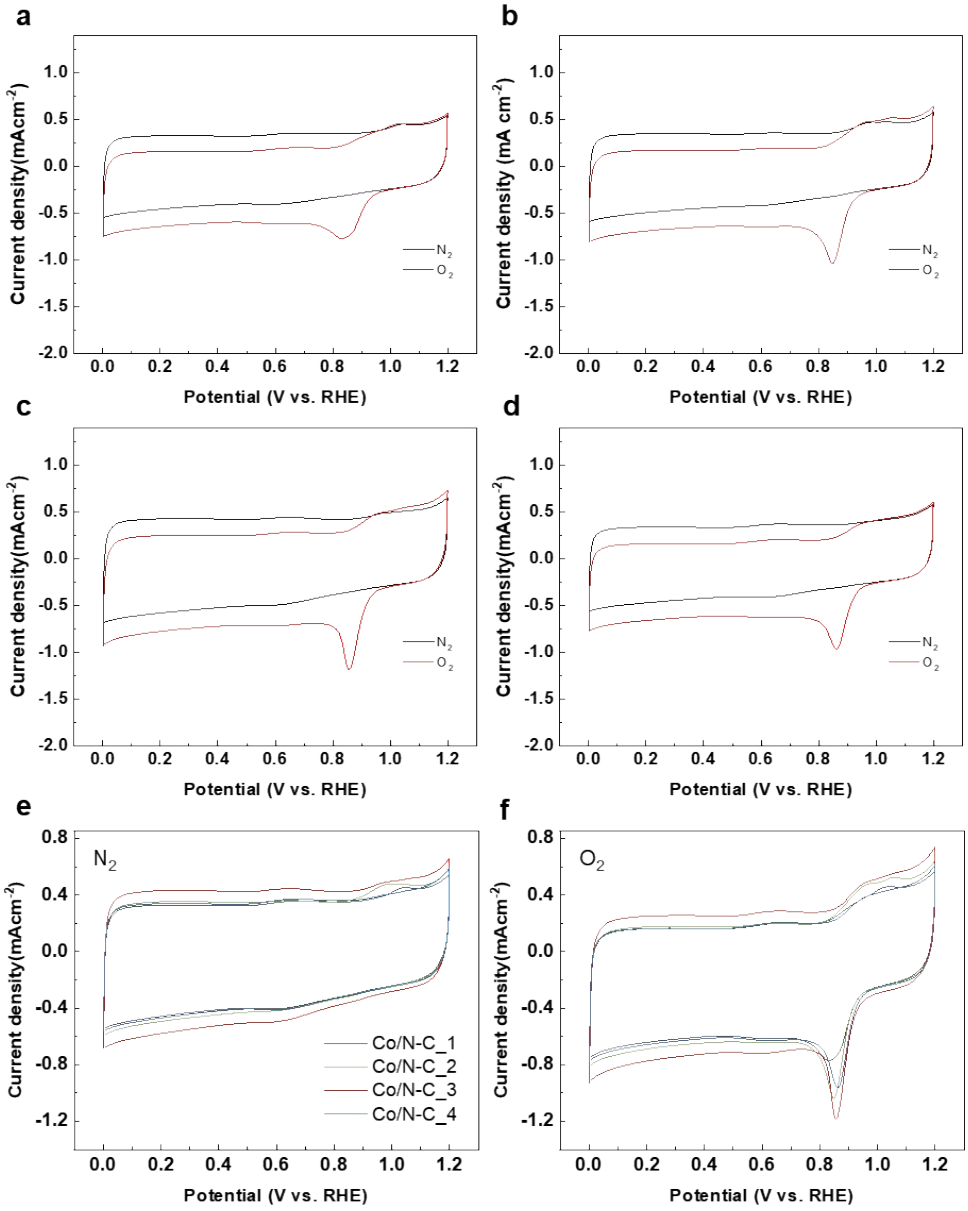

Figure. S11. CV curves of (a) Co/N-C_1, (b) Co/N-C_2, (c) Co/N-C_3, and (d) Co/N-C_4 in 0.1 M KOH solution at 5 mV s^{-1} within a potential window from 0 to 1.2 V. Comparison of CV curves in (e) N_2-saturated and (f) O_2-saturated electrolytes.

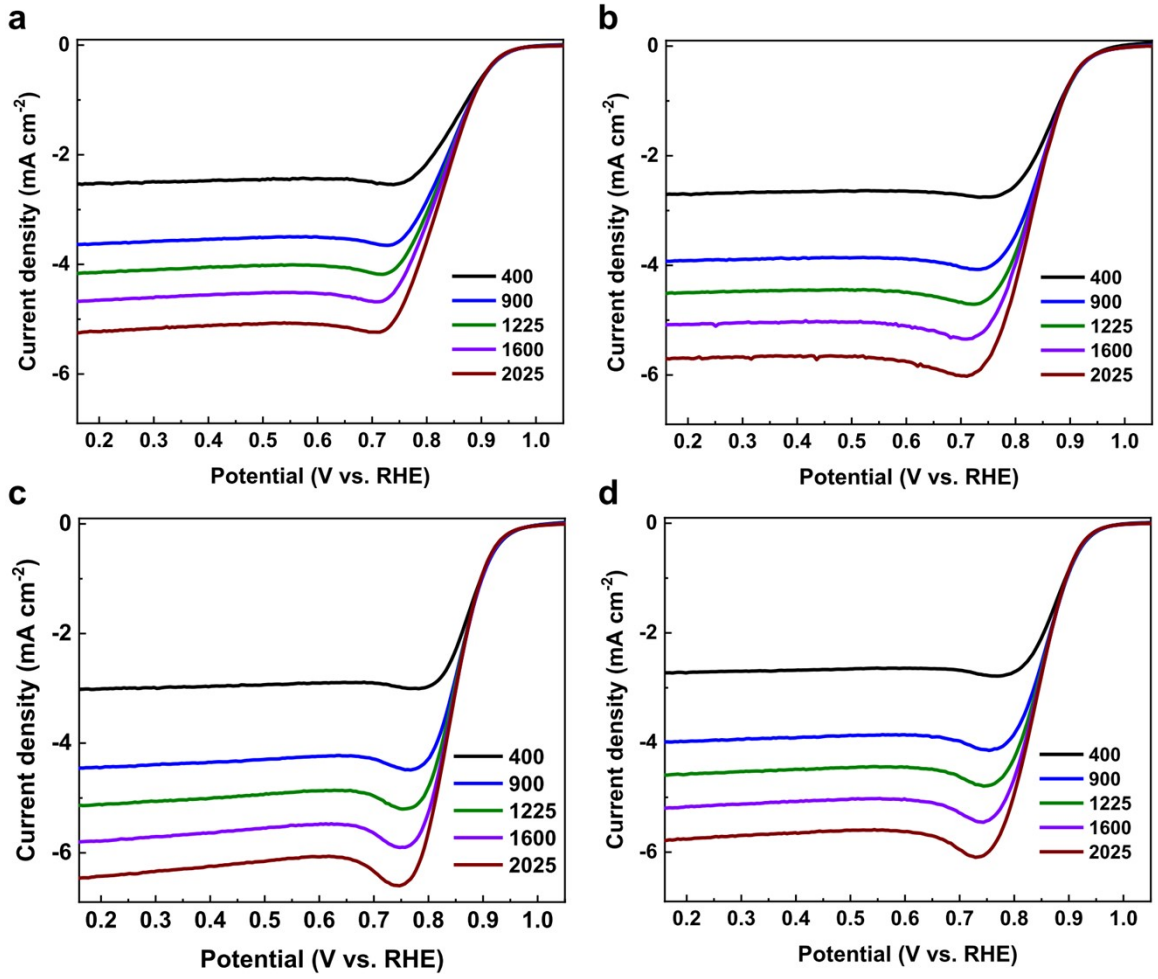

Figure. S12. LSV curves of (a) Co/N-C_1, (b) Co/N-C_2, (c) Co/N-C_3, and (d) Co/N-C_4 in 0.1 M KOH solution at various rotating speed (400, 900, 1225, 1600, 2025 rpm).

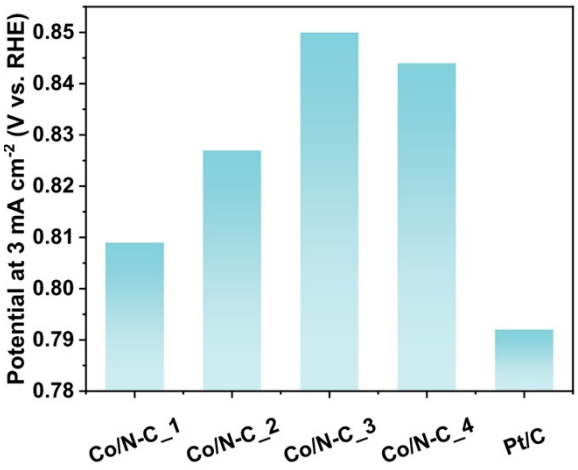

Figure. S13. The half-wave potential (V vs. RHE at 3 mA cm^{-2}) of Co/N-C_1, Co/N-C_2, Co/N-C_3, Co/N-C_4, and Pt/C.

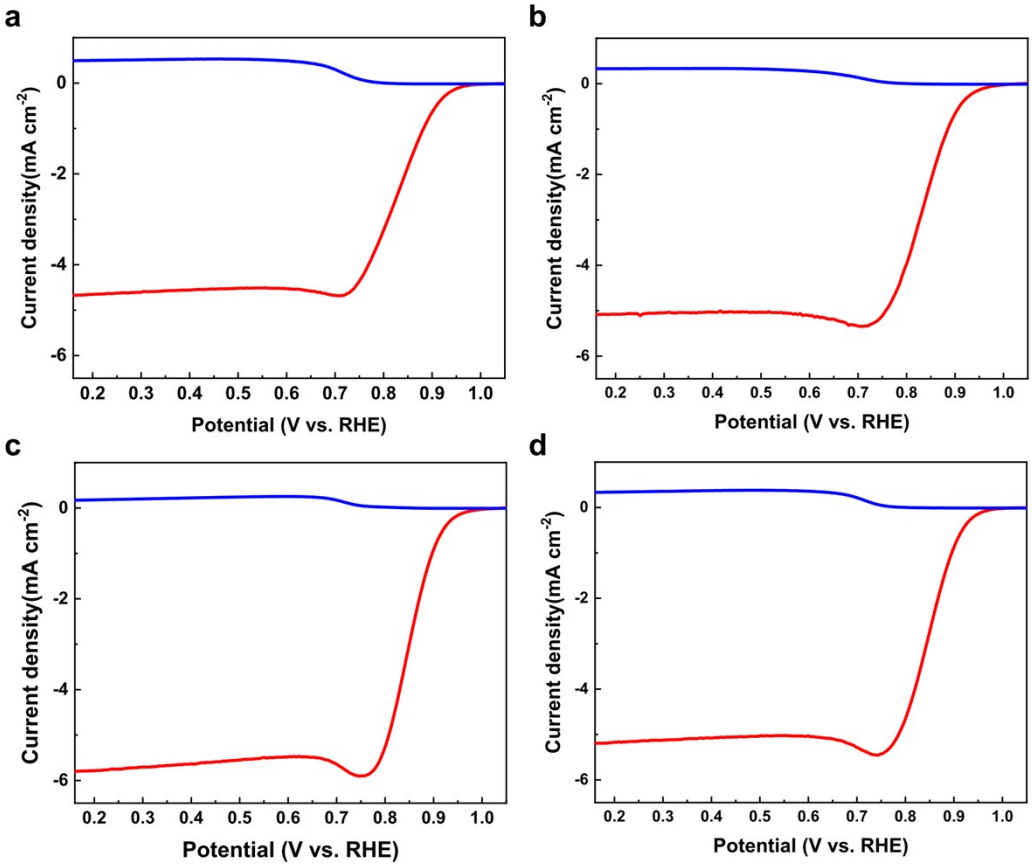

Figure. S14. RRDE curves of (a) Co/N-C_1, (b) Co/N-C_2, (c) Co/N-C_3, and (d) Co/N-C_4 in 0.1 M KOH solution at 1600 rpm, scan rate 5 mV s^{-1}.

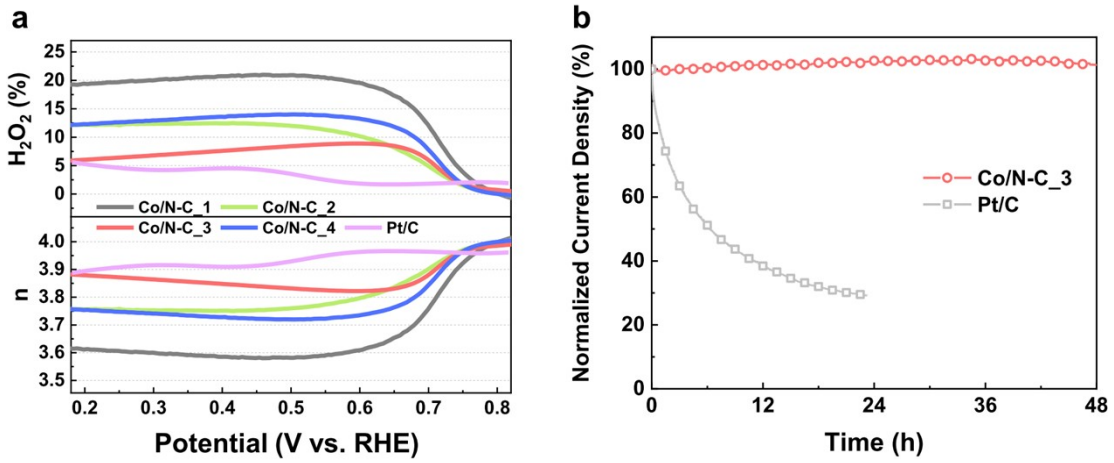

Figure. S15. (a) Hydrogen peroxide yield and electron transfer number of Co/N-C series and Pt/C. (b) Normalized chronoamperometric current density at 0.6 V (vs. RHE) of Co/N-C_3 and Pt/C.

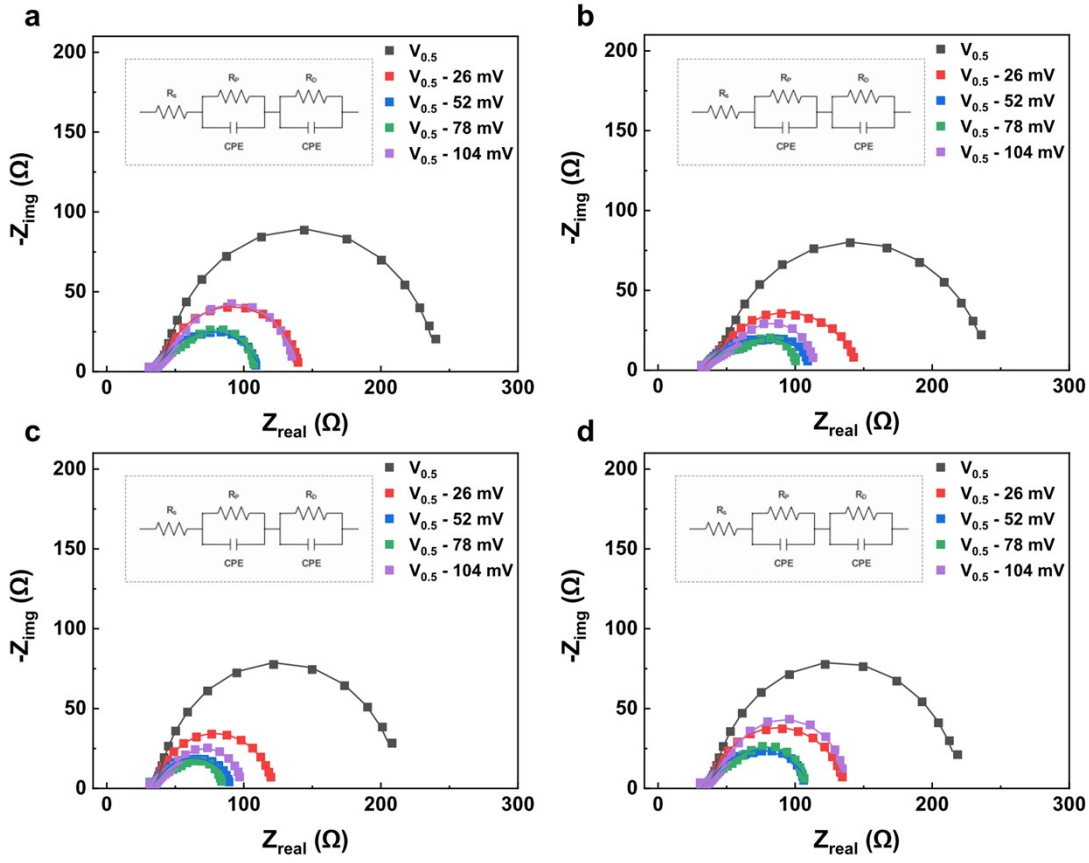

Figure. S16. EIS curves of (a) Co/N-C_1, (b) Co/N-C_2, (c) Co/N-C_3, and (d) Co/N-C_4 in 0.1 M KOH solution at the various potentials.

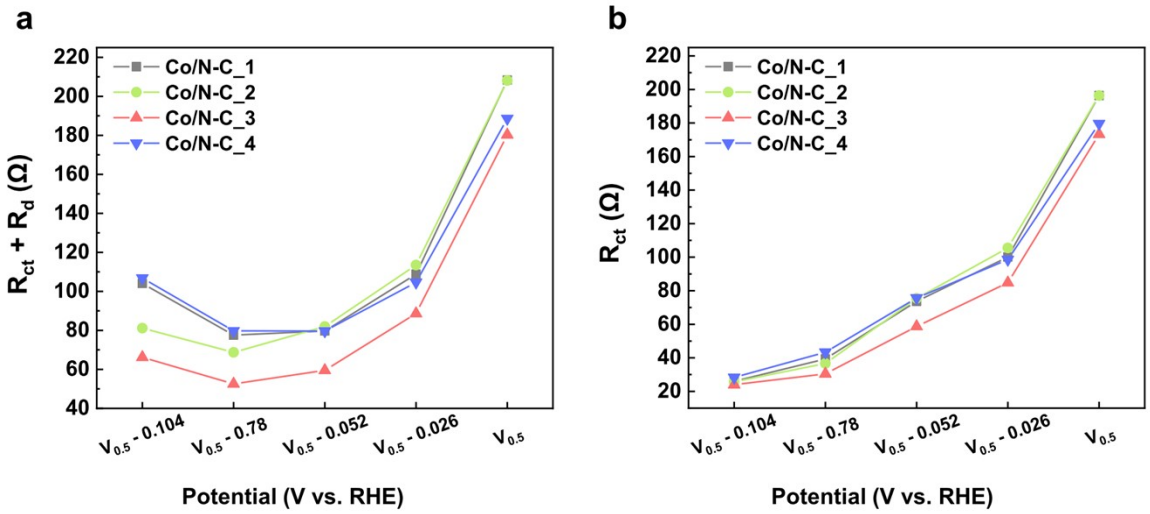

Figure. S17. (a) The sum of charge transfer (R_{ct}) and mass transfer resistance (R_d) and (b) charge transfer resistance calculated from impedance spectra at different potential of Co/N-C series

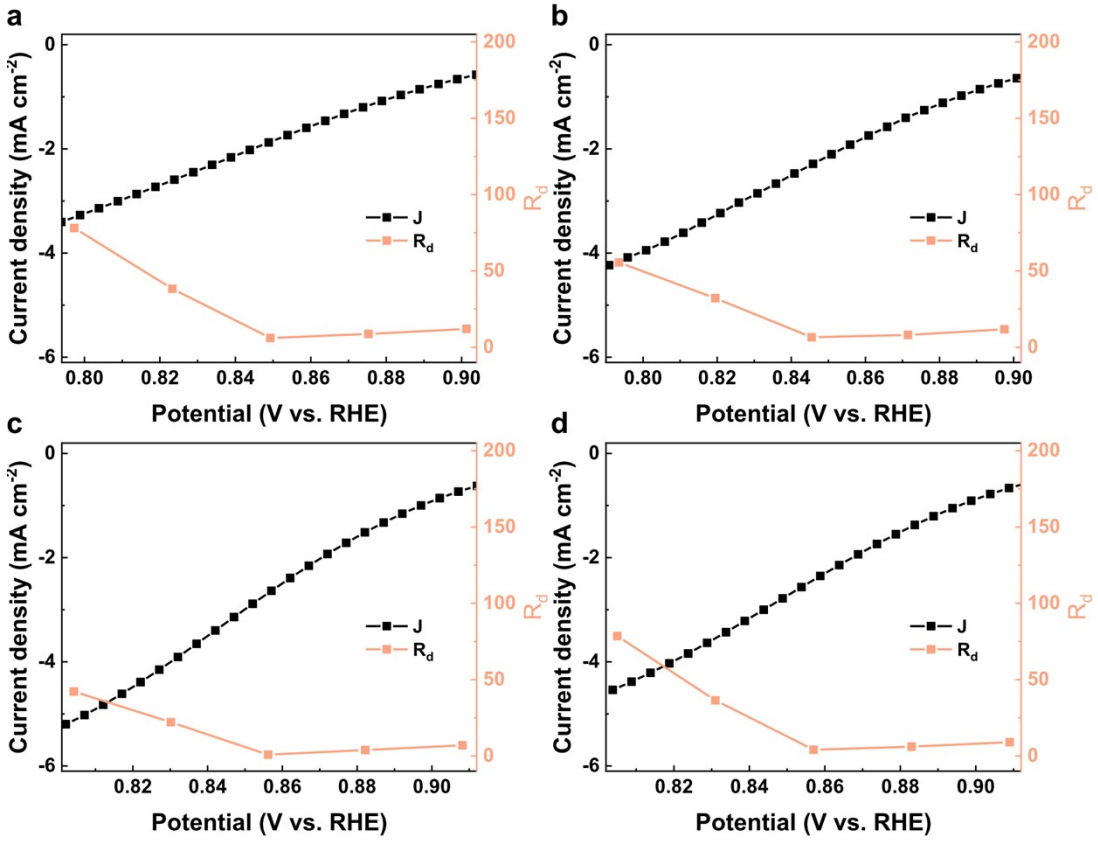

Figure. S18. LSV and mass transfer resistance of (a) Co/N-C_1, (b) Co/N-C_2, (c) Co/N-C_3, and (d) Co/N-C_4 in 0.1 M KOH solution at 1600 rpm.

Table S1. Pore surface area results of oxidized ZIFs.

Sample	Surface area (cm^2 g^{-1})	
	V_{tot}	V_{meso}
ZIF	1.60	1.02
O-ZIF@280	1.61	1.11
O-ZIF@310	1.61	1.22
O-ZIF@340	1.07	1.00

Table S2. Elemental quantification defined by using XPS of oxidized ZIF.

Sample	C (at%)	N (at%)	O (at%)	Co (at%)	Zn (at%)
ZIF	59.47	25.53	5.57	1.06	8.38
O-ZIF@280	58.32	24.65	7.96	0.89	8.18
O-ZIF@310	54.40	25.23	11.06	1.28	8.03
O-ZIF@340	50.30	24.38	14.43	1.23	9.67

Table S3. Bulk Co and Zn contents of the ZIF-derived catalysts determined by ICP-OES.

Sample	Oxidation Temp. (°C)	Co (wt.%)	Zn (wt.%)
Co/N-C_1		8.83	2.92
Co/N-C_2	280	11.54	1.16
Co/N-C_3	310	13.06	4.93
Co/N-C_4	340	10.51	2.5

Table S4. Comparison of the ORR performance of the optimized Co/N-C catalyst with recently reported MOF-derived transition metal/nitrogen-doped carbon (TM/N-C) catalysts.Note: E_{onset} and $E_{1/2}$ represent the onset and half-wave potentials of the reported catalysts, respectively. Values in parentheses refer to the commercial Pt/C tested under the same conditions in each study. The potential differences (ΔE_{onset} and $\Delta E_{1/2}$) were calculated by subtracting the Pt/C value from the main sample value (E_{sample}-$E_{Pt/C}$) to provide a normalized comparison of intrinsic activity.

Electrocatalysts	E_{onset}	E_{onset} (Pt/C)	ΔE_{onset}	E_{half}	$E_{half\ (Pt/C)}$	$\Delta E_{1/2.}$	Stability (Current retention@operating time)	Ref.
Co/N-C_3	0.963	0.938	**0.025**	0.85	0.792	**0.058**	**~100% @172,800 s**	This work
CoFe@CNT	0.93	0.97	-0.04	0.85	0.83	0.02	92% @20,000 s	1
Co/NHCNT-160	0.955	0.96	-0.005	0.88	0.82	0.06	99.70% @25,000 s	2
Co–N/PCNs-2	0.99	0.98	0.01	0.88	0.85	0.03		3
CoCu-NPC-1000	0.988	0.982	0.006	0.849	0.867	-0.018	92.29% @36,000 s	4
FeCo@NC-II	0.999	0.995	0.004	0.907	0.867	0.04	81% @80,000 s	5
Fe3C-Co-NC	1.02	0.97	0.05	0.89	0.86	0.03	97% @25,000 s	6
FeCo@CNTs-60	1.05	1.05	0	0.95	0.95	0		7
ZIF-67–6	0.9	0.89	0.01	0.83	0.83	0	92.11% @10,000 s	8
Fe@NSC	0.96	0.93	0.03	0.87	0.83	0.04	86.5% @10,000 s	9
Co@MNC-20	0.963	0.97	-0.007	0.87	0.843	0.027		10
Fe/N@CNT	1.069	1	0.069	0.892	0.858	0.034	93.9% @36,000 s	11

Table S5. Summary of parameters for kinetic current (J_k), mass activity (MA), and Apparent TOF calculation.

Sample	J@0.8 V (mA cm^{-2})	J_{diff}@0.4V (mA cm^{-2})	J_k@0.8 V (mA cm^{-2})	Catalyst loading (mg cm^{-2})	Co Content (wt%)	MA_{catal} (A g$^{-1}_{catal}$)	MA_{metal} (A g$^{-1}_{Co}$)	Apparent TOF (s^{-1})
Co/N-C_1	3.23	4.56	11.07	0.1	8.83	29.22	330.96	0.0505
Co/N-C_2	3.96	5.03	18.62	0.379	11.54	49.12	425.59	0.065
Co/N-C_3	5.26	5.64	78.07	0.379	13.06	205.98	1577.45	0.2409
Co/N-C_4	4.66	5.08	56.36	0.379	10.51	148.71	1415.38	0.2161
Pt/C	2.71	5.23	5.62	0.379	20	56.24	281.22	0.1421

Reference

1. Z. Fu, H. Zhuo, X. Liu, W. Li, H. Song, Z. Shi, L. Feng, T. Jin, W. Chen and Y. Chen, *ACS Appl. Energy Mater.*, **2025**, 8, 1051–1059.

2. X. He, L. Chang, P. Han, K. Li, H. Wu, Y. Tang, F. Gao, Y. Zhang and A. Zhou, *Colloids Surf. A*, **2023**, 663, 130988.

3. Y. Zhu, Z. Zhang, Z. Lei, Y. Tan, W. Wu, S. Mu and N. Cheng, *Carbon*, **2020**, 167, 188–195.

4. X. Qu, M. Wang, D. Yang, Y. Wu, X. Guo, X. Liu, H. Yang and Y. Wen, *J. Mater. Sci.*, **2024**, 59, 19785–19796.

5. Q. Wang, L. Wang, S. Zhang, Z. Chen, W. Peng, Y. Li and X. Fan, *J. Colloid Interface Sci.*, **2025**, 677, 800–811.

6. H. Wang, C. Sun, E. Zhu, C. Shi, J. Yu and M. Xu, *J. Alloys Compd.*, **2023**, 948, 169728.

7. C. Fang, X. Tang and Q. Yi, *Appl. Catal. B*, **2024**, 341, 123346.

8. Y. Ju, W. Huang, Z. Gao, M. Liu and N. Huang, *Appl. Mater. Today*, **2025**, 42, 102576.

9. D. Liu, K. Srinivas, F. Ma, H. Yu, Z. Zhang, M. Wang, Y. Wu and Y. Chen, *J. Alloys Compd.*, **2023**, 937, 168496.

10. X. Liu, Y. Zhao, J. Wei, X. Song, Y. Asakura and Y. Yamauchi, *Chem. Eng. J.*, **2025**, 520, 165277.

11. Z. Wang, X. Meng, H. Wang, L. Bao, C. Li, Y. Cong and Q. Zhao, *Int. J. Electrochem. Sci.*, **2023**, 18, 100131.